

**Supporting-information for**  
**Weak Fermi level pinning induced adsorption energy**  
**non-charge-transfer mechanism during O<sub>2</sub> adsorption in**  
**silicene/graphene heterojunction**

Xuhong Zhao, Haiyuan Chen, Jianwei Wang,\* and Xiaobin Niu\*

*School of Materials and Energy, University of Electronic  
Science and Technology of China, Chengdu 611731, China*

**Adsorption energy and work function:**

The results have shown in Table 1 and Fig. 2. ( $\Delta E$  means the difference between the graphene/silicene adsorption energy and the silicene adsorption energy). The energy results show that O<sub>2</sub> has a more significant adsorption capacity for silicene, and the adsorption energy reaches up to about 3 eV, while the adsorption capacity of H<sub>2</sub>O, N<sub>2</sub>, and H<sub>2</sub> on silicene is very weak. The reason for this result may be that the production of oxygen adsorption on silicene is very stable SiO<sub>2</sub>, which further leads to the cracking of silicene and lower its stability. And silicene is not sensitive to H<sub>2</sub>O, N<sub>2</sub>, and H<sub>2</sub> in the air. Therefore, in the follow-up studies on the stability of silicene, we will focus on oxygen adsorption to explore the stability of silicene.

In the process of calculating the work function, as shown in Fig. 2, the  $\Phi$  is affected by the different Fermi level energies and the semiconductor energy band edges in the heterojunction

$$\begin{aligned}\Phi_e &= W - E_{ea} \\ \Phi_h &= E_{ip} - W\end{aligned}\tag{1}$$

Where  $W$  represents the work function of the metal, and  $E_{ea}$  and  $E_{ip}$  respectively represent the electron affinity and ionization potential of the semiconductor [1].

The construction of heterojunction is realized after following steps. In order to search the effects of gas molecules absorbing on the surface of graphene/silicene, in comparison to that of silicene, we keep the silicene ( $a=b=3.85$  Å) unmoved while rotating the graphene ( $a=b=2.45$  Å), and then two independent monolayers were compounded together to compensate for lattice mis-match. Finally, we choose two monolayer materials with a turning angle of 14.07° and a space of 3.6 Å between the layer after optimization, and the mismatch between the two monolayers meets the requirements. On this basis, we completed the construction of the silicene

model. In the process of establishing a twist angle heterojunction [2], since silicene has a honeycomb structuresimilar to graphene (Fig. 3), we assume that its lattice constant is  $a$ , and the primitive cell base vector can be expressed as:

$$\begin{aligned}\mathbf{a}_1 &= a\mathbf{e}_x & (2) \\ \mathbf{a}_2 &= -\frac{1}{2}a\mathbf{e}_x + \frac{\sqrt{3}}{2}a\mathbf{e}_y & (3)\end{aligned}$$

$\mathbf{e}_x$  and  $\mathbf{e}_y$  are unit vectors along the x-axis and y-axis in rectangular coordinates.

The transformation relationship between silicene supercell base vector and primitive cell base vector is expressed as:

$$\begin{pmatrix} \mathbf{A}_1 \\ \mathbf{A}_2 \end{pmatrix} = \begin{pmatrix} M_{11} & M_{12} \\ M_{21} & M_{22} \end{pmatrix} \begin{pmatrix} \mathbf{a}_1 \\ \mathbf{a}_2 \end{pmatrix}$$

$M_{ij}$  is an integer.  $\det M = \begin{vmatrix} M_{11} & M_{12} \\ M_{21} & M_{22} \end{vmatrix} = N$  is the number of primitive cells contained in the supercell,

as shown in Fig. 6. Obviously,  $\mathbf{A}_1 = i\mathbf{a}_1$ .

In the same way, we set the unit cell base vectors of graphene as  $\mathbf{b}_1$  and  $\mathbf{b}_2$ , and also  $\mathbf{B}_1 = g\mathbf{b}_1$ .

Because in the heterogeneous structure,  $|\mathbf{A}_1| = |\mathbf{B}_1|$ . In the structure file, we can easily get  $\mathbf{a}_1$  and  $\mathbf{b}_1$ , then the rotation angle between two supercells is expressed as:

$$\cos \theta = \frac{\mathbf{A}_1 \cdot \mathbf{B}_1}{|\mathbf{A}_1||\mathbf{B}_1|} = \frac{\mathbf{a}_1 \cdot \mathbf{b}_1}{|\mathbf{a}_1||\mathbf{b}_1|} \quad (3)$$

TABLE 1. The table shows the adsorption energy of graphene/silicene and silicene and their comparison.

System	$E_{\text{tot}}$ (eV)	$E_{\text{ad}}$ (eV)	System	$E_{\text{tot}}$ (eV)	$E_{\text{ad}}$ (eV)	$\Delta E$
graphene/silicene	-880.840		silicene	-155.069		0.307
graphene/silicene-O <sub>2</sub>	-892.702	2.910	silicene-O <sub>2</sub>	-167.009	3.275	0.365
graphene/silicene-H <sub>2</sub> O	-895.208	0.146	silicene-H <sub>2</sub> O	-169.455	0.149	0.003
graphene/silicene-N <sub>2</sub>	-897.520	0.073	silicene-N <sub>2</sub>	-171.749	0.073	0.000
graphene/silicene-H <sub>2</sub>	-887.636	0.101	silicene-H <sub>2</sub>	-161.869	0.105	0.004

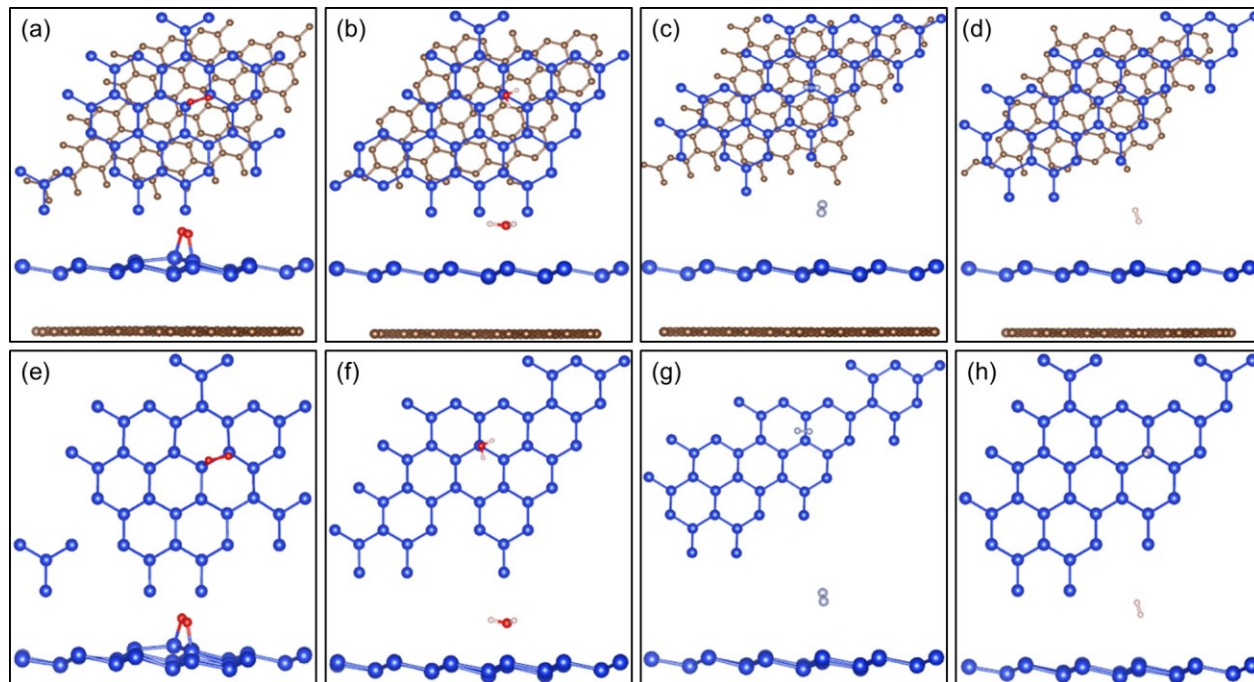


FIG. 1. Schematic views of the heterojunction and the silicene (top and side view), (a~h) is the structure of gas molecules ( $O_2$ ,  $H_2O$ ,  $N_2$ , and  $H_2$ ) adsorbed on the graphene/silicene and silicene. The blue, brown, red, grey, and white balls represent Si, C, O, N, and H atoms, respectively.

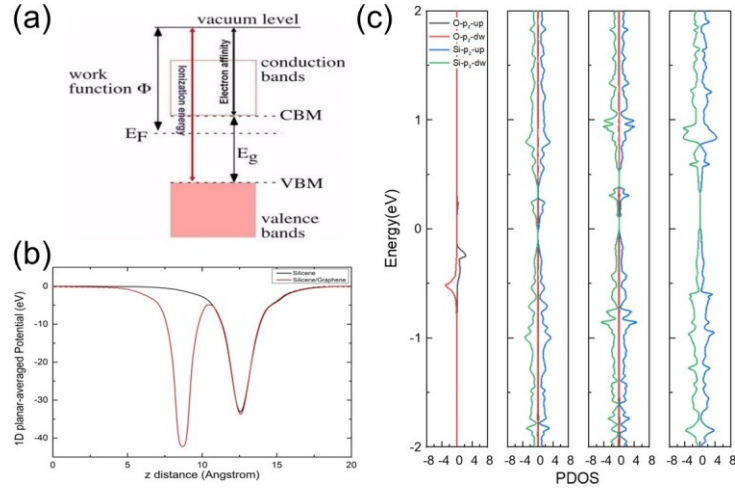


FIG. 2. (a) Band composition of materials. (b) The planar-average potential of silicene and silicene/graphene. (c) The PDOS of the  $p_z$  orbitals of Si atoms and O atoms in pure oxygen, oxygen-absorbing heterostructure, oxygen-absorbing pure silicene, and pure silicene are shown in sequence.

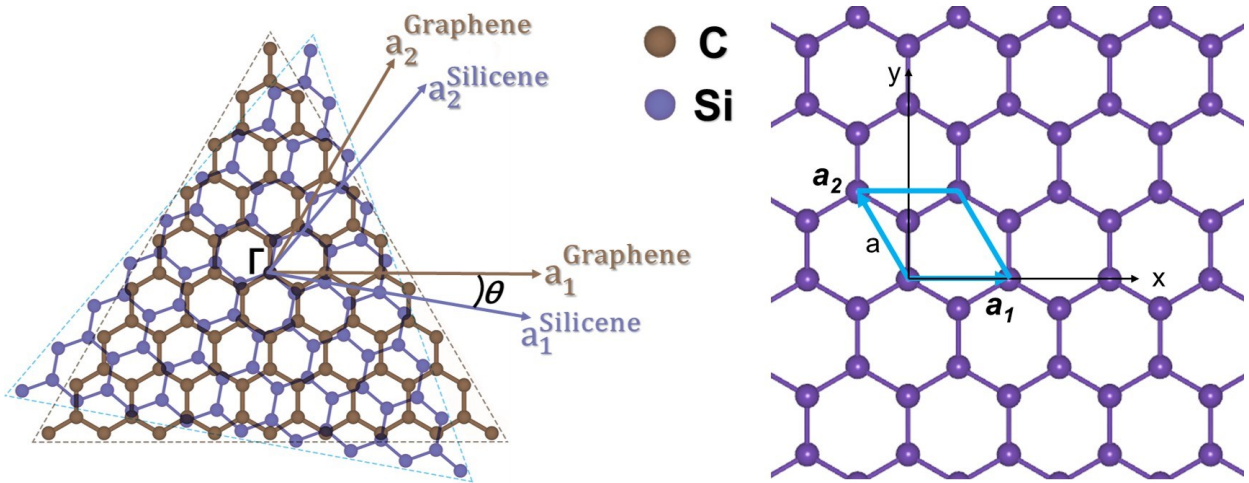


FIG. 3. The structure of twist angles heterojunction. (Purple and grey color represent Si and C atoms, respectively.) The structure of silicene  $a$  is the lattice constant, the parallelogram represents the primitive cell, and the blue arrows represent the two basis vectors  $a_1$  and  $a_2$  of the primitive cell.

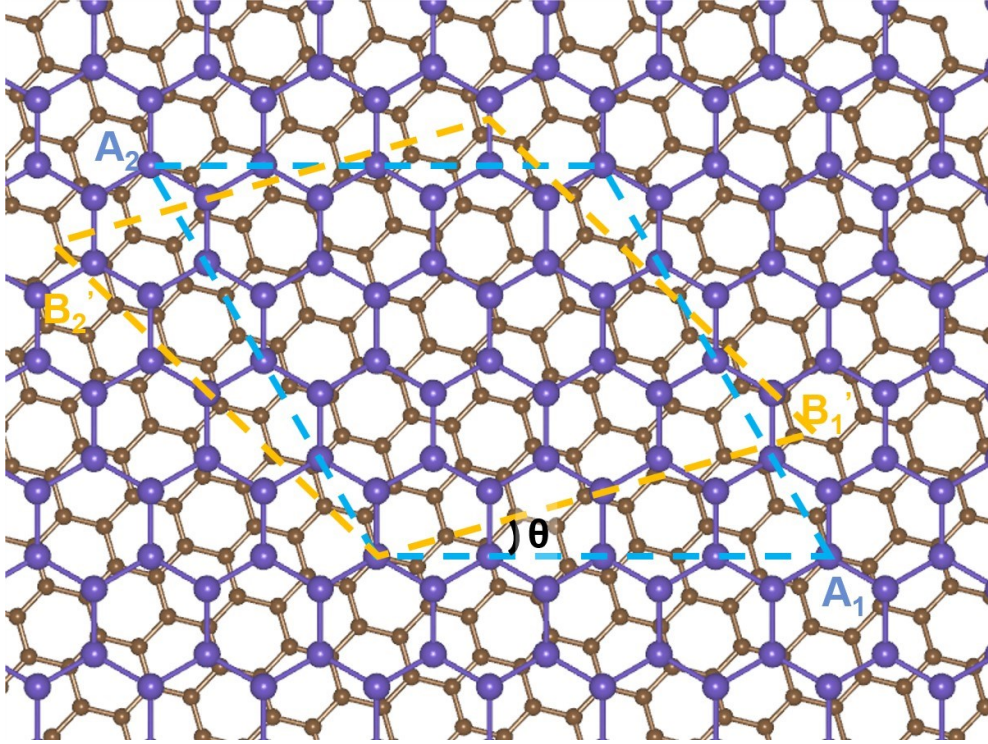


FIG. 4. The structure of the twist angle silicene/graphene heterojunction, the blue and yellow parallelograms represent the silicene and graphene supercells, respectively.  $\theta$  is the relative twist angle of the two supercells.

TABLE 2. The table shows the adsorption energy and work function of twist angle graphene/silicene and silicene and their comparison.

<b>Twist angle (°)</b>	$E_{\text{ad-hetero}}$	$E_{\text{ad-silicene}}$ (eV)	$\Delta E$ (eV)	$\Phi_{\text{hetero}}$	$\Phi_{\text{silicene}}$	$\Delta\Phi$
0.80	3.143	3.366	0.223	4.443	4.750	0.307
2.16	2.917	3.367	0.450	4.463	4.757	0.294
4.17	1.977	2.303	0.326	4.430	4.787	0.357
5.68	3.198	3.288	0.090	4.323	4.797	0.474
5.84	2.902	3.215	0.313	4.530	4.877	0.347
14.07	2.910	3.275	0.365	4.477	4.837	0.360
24.34	2.911	3.216	0.304	4.527	4.841	0.314
25.54	2.915	3.363	0.448	4.401	4.896	0.495
27.13	2.882	3.436	0.554	4.470	4.753	0.283
31.82	2.930	3.421	0.491	4.510	4.761	0.251
35.78	2.906	3.434	0.529	4.464	4.752	0.288
35.89	2.911	3.215	0.303	4.567	4.873	0.306
36.37	2.917	3.364	0.447	4.427	4.756	0.329
36.88	3.047	3.368	0.321	4.396	4.747	0.351
41.83	2.908	3.273	0.365	4.538	4.851	0.313
45.97	3.047	3.209	0.163	4.465	4.883	0.418
52.88	3.264	3.332	0.069	4.401	4.797	0.396
54.32	3.303	3.342	0.039	4.506	4.828	0.322
57.74	2.902	3.362	0.461	4.374	4.756	0.382
58.86	2.903	3.210	0.308	4.567	4.850	0.283

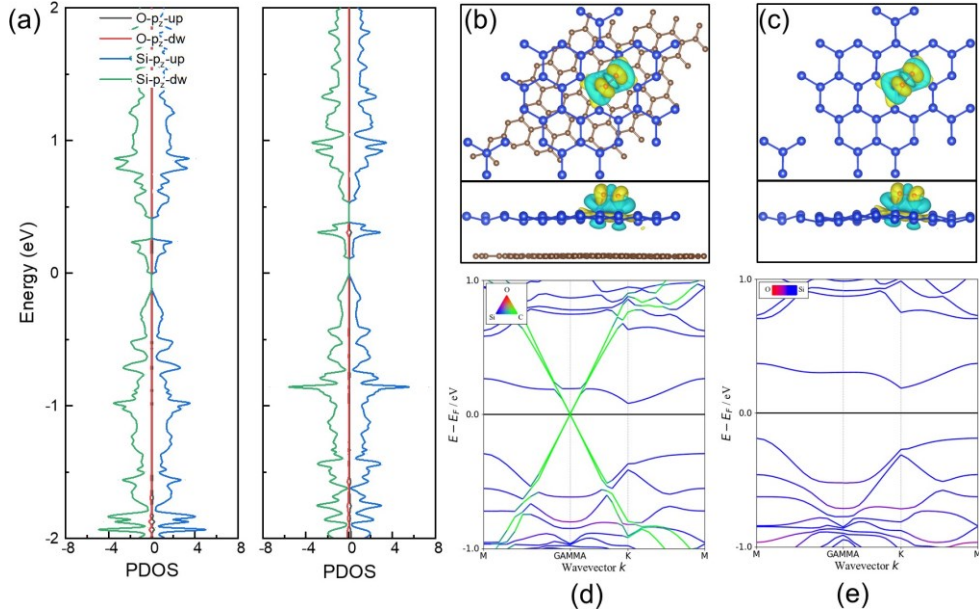


FIG. 5. (a) The PDOS of the  $p_z$  orbitals of Si atoms and O atoms in oxygen-absorbing heterojunction and oxygen-absorbing pure silicene are shown in sequence. (b-c) Charge density Difference diagram of heterojunction and pure silicene after adsorbing oxygen. (d-e) Band structure of heterojunction and pure silicene after adsorbing oxygen.

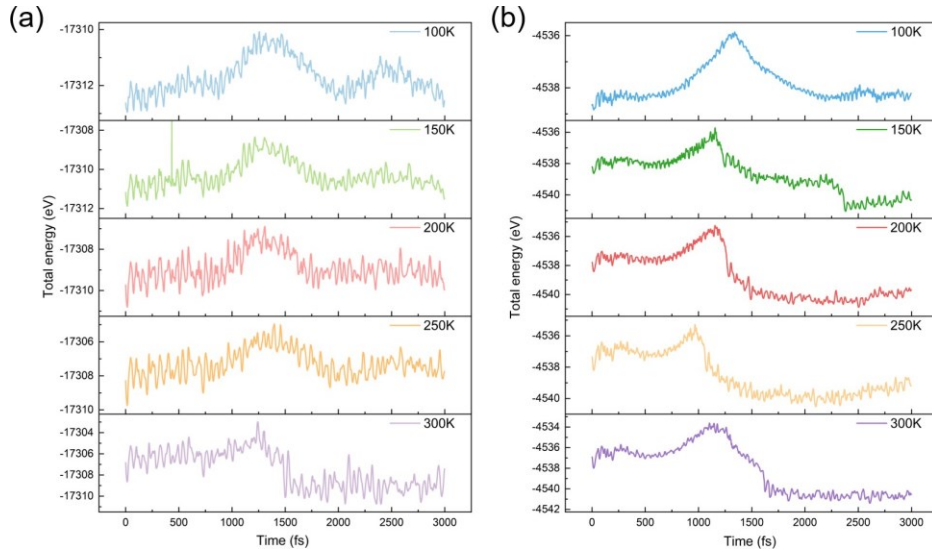


FIG. 6. Total energy changes of SGH (a) and PS (b) at different temperatures.

TABLE 3. The amount of electron transfer of twist angle heterojunction and silicene.

Twist angle ( $^{\circ}$ )	$q_{\text{hetero}}$ (eV)	$q_{\text{silicene}}$ (eV)
0.80	-1.6981	-1.5855
2.16	-1.5580	-1.6315
4.17	-1.5506	-1.6003
5.68	-1.6875	-1.6722
5.84	-1.6148	-1.5398
14.07	-1.6099	-1.6578
24.34	-1.6043	-1.6653
25.54	-1.6822	-1.6351
27.13	-1.5713	-1.7239
31.82	-1.5476	-1.5212
35.78	-1.6086	-1.7697
35.89	-1.6169	-1.6313
36.37	-1.6577	-1.4950
36.88	-1.5752	-1.4439
41.83	-1.5862	-1.6386
45.97	-1.6457	-1.6130
52.88	-1.6597	-1.5799
54.32	-1.6802	-1.5802
57.74	-1.5281	-1.4750
58.86	-1.6308	-1.4913

- 
- [1] Y. Liu, P. Stradins, and S.-H. Wei, *Science advances* **2**, e1600069 (2016).
- [2] J. Wang, M. Ge, R. Ma, Y. Sun, L. Cheng, R. Wang, M. Guo, and J. Zhang, *Journal of Applied Physics* **131**, 034301 (2022).